Electronic Supplementary Material (ESI) for Journal of Materials Chemistry A.
This journal is © The Royal Society of Chemistry 2019

Suit the Hydrogel with Armor: Strong and Super Tough Biomass Reinforced Hydrogel with Excellent Conductivity and Anti-bacterial Performance

Xiao Zhang[a§], Weifeng Liu*[§], Junqi Cai[a], Jinhao Huang[a], Xueqing Qiu*[ab]

[a] School of Chemistry and Chemical Engineering, Guangdong Engineering Research Center for Green Fine Chemicals, South China University of Technology, Wushan Road 381, Guangzhou, Guangdong, 510640, China

[b] State Key Laboratory of Pulp and Paper Engineering, South China University of Technology, Wushan Road 381, Guangzhou, Guangdong, 510640, China

[§] These authors contributed equally.

*Corresponding authors

E-mail: weifengliu@scut.edu.cn (W. Liu); cexqqiu@scut.edu.cn (X. Qiu)

Tel.: +86 020-87114722

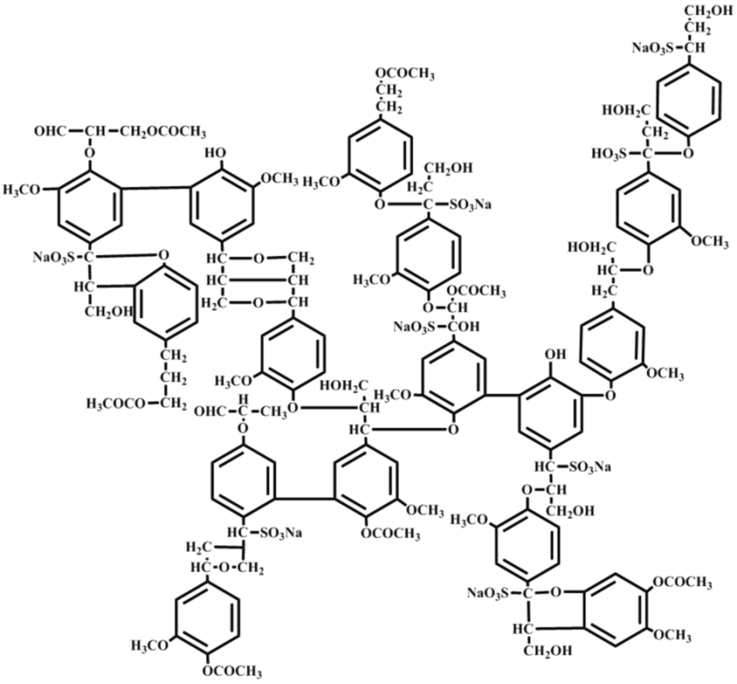

Figure S1. The possible molecular structure of LS.

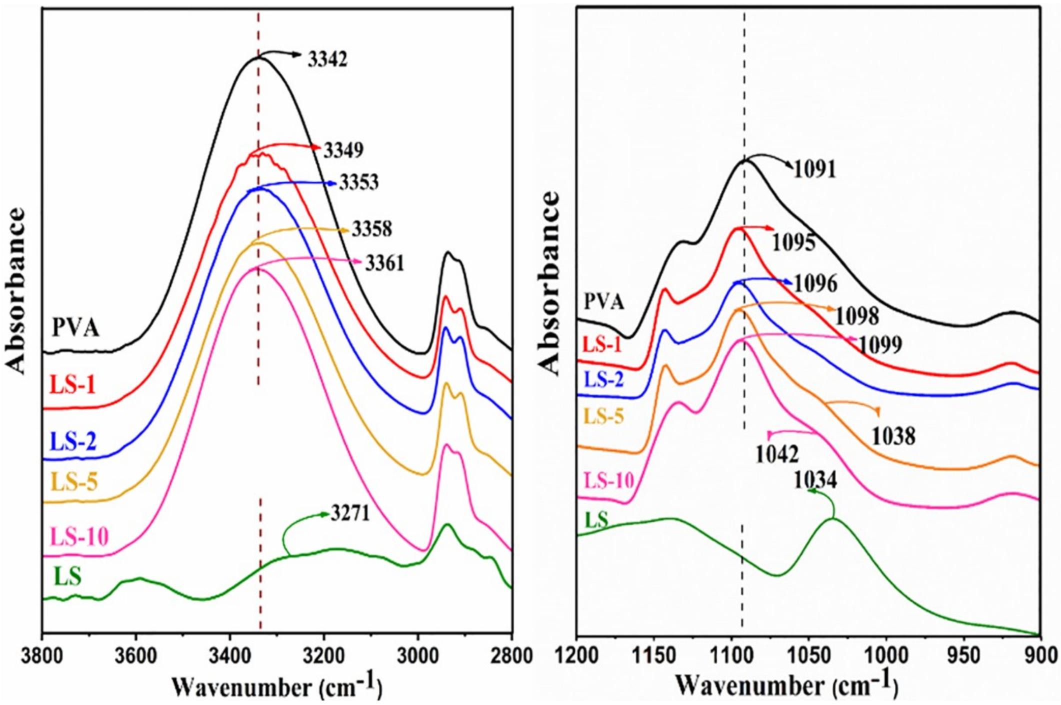

(a) (b)

Figure S2. FTIR spectra of PVA, LS and PVA/LS nanocomposites hydrogel showing the variations of a) O–H and b) C–O or S–O stretching vibrations.

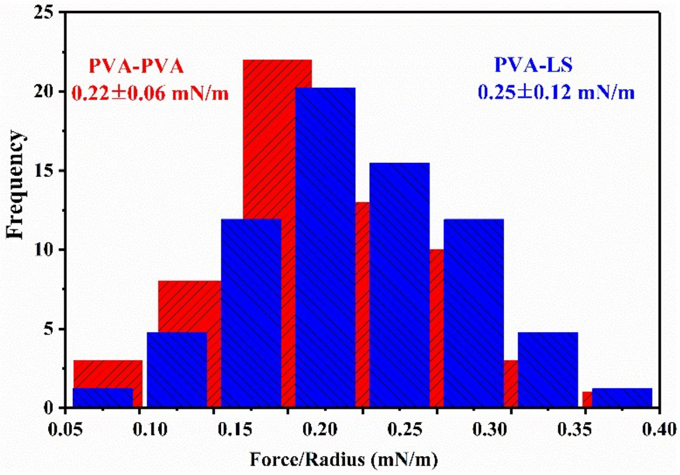

Figure S3. Comparison of interaction forces between PVA- PVA and PVA- LS.[1]

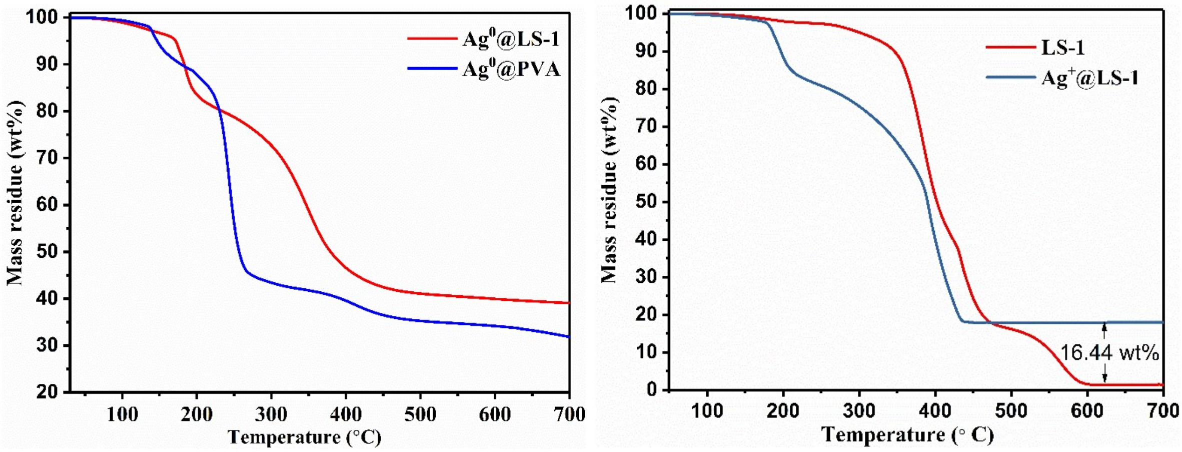

(a) (b)**Figure S4.** a) TG curves of PVA composite hydrogels for Ag^0@LS-1 and Ag^0@PVA at N_2 atmosphere, the concentration of $AgNO_3$ was 0.5 M and the soaking time was 4 h; the $Na_3C_6H_5O_7$ concentration was 1.0 M and the soaking time was 1 h. Ag^0@PVA was prepared without LS for comparison; b) TG curves of LS-1 and Ag$^+$@LS-1 at air atmosphere.

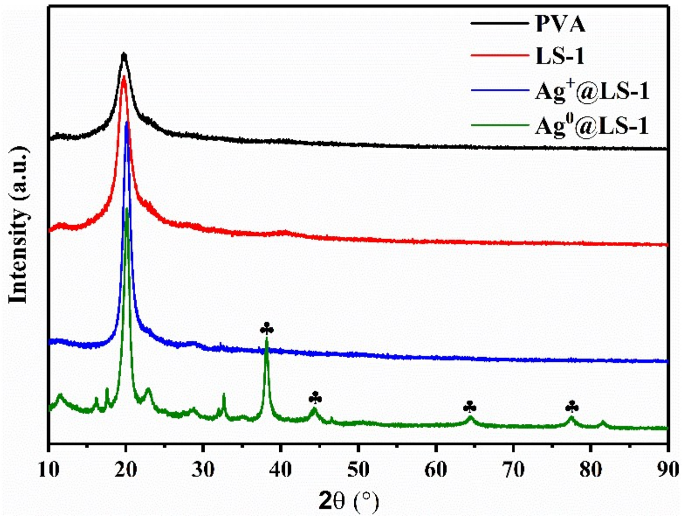

Figure S5. XRD pattern of pure PVA and PVA nanocomposite hydrogels.

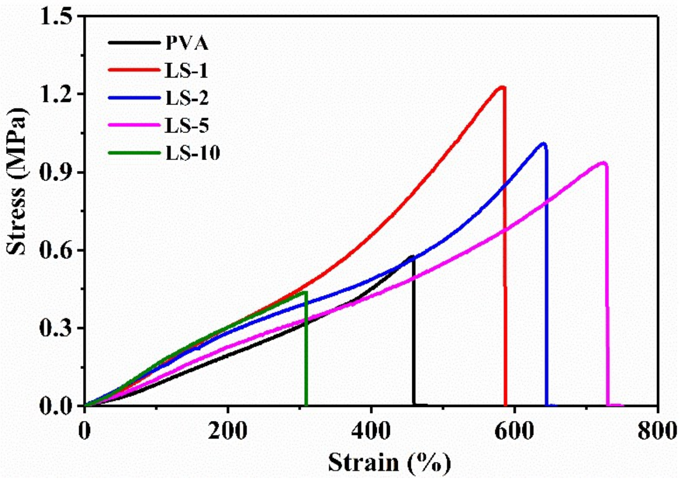

Figure S6. Uniaxial tensile curves of PVA/LS composite hydrogels in comparison with pure PVA hydrogel.

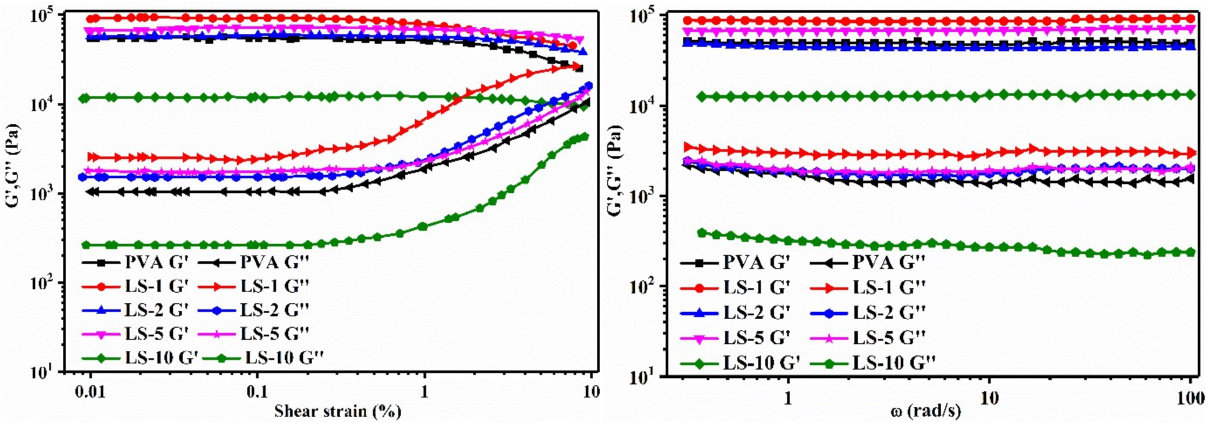

(a) (b)

Figure S7. a) Shear strain dependence of shear storage modulus (G') and loss modulus (G'') of PVA hydrogel and PVA/LS composite hydrogels at different LS loadings; b) Angular frequency dependence of shear storage modulus (G′) and loss modulus (G″) of PVA hydrogel and PVA/LS composite hydrogels at different LS loadings.

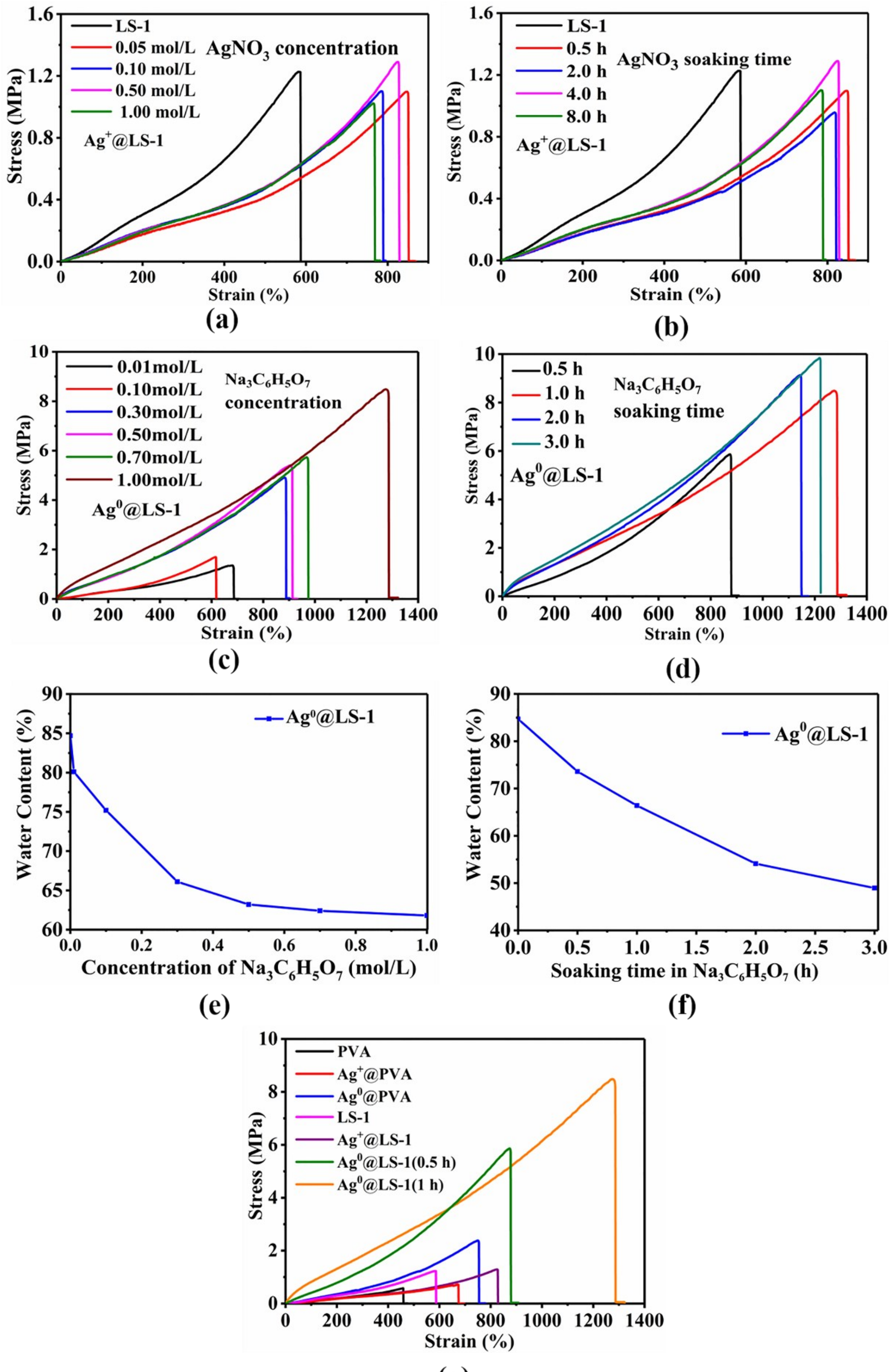

Figure S8. Comparison of uniaxial tensile curves for Ag$^+$@LS-1 in different AgNO$_3$ concentrations with constant soaking time of 4 h a) and different soaking time in constant AgNO$_3$ concentration of 0.5 M b); Comparison of uniaxial tensile curves for Ag^0@LS-1 in different Na$_3$C$_6$H$_5$O$_7$ concentrations with constant soaking time of 1 h c) and different soaking time in constant Na$_3$C$_6$H$_5$O$_7$ concentration of 1.0 M d); e) Na$_3$C$_6$H$_5$O$_7$ concentration dependence of water content for Ag^0@LS-1 with constant soaking time of 1 h; f) Soaking time dependence of water content for Ag^0@LS-1 in constant sodium citrate concentration of 1.0 M; g) Comparison of uniaxial tensile curves of pure PVA and PVA nanocomposite hydrogels; Ag$^+$@PVA was prepared by soaking the pristine PVA hydrogel in $Na_3C_6H_5O_7$ solution directly; for Ag$^+$@LS-1 and Ag$^+$@PVA, the concentration of $AgNO_3$ was 0.5 M and the soaking time was 4 h; for Ag^0@LS-1(1 h) and Ag^0@PVA, the $Na_3C_6H_5O_7$ concentration was 1.0 M and the soaking time was 1 h; for Ag^0@LS-1(0.5 h), the $Na_3C_6H_5O_7$ concentration was 1.0 M and the soaking time was 0.5 h.[2]

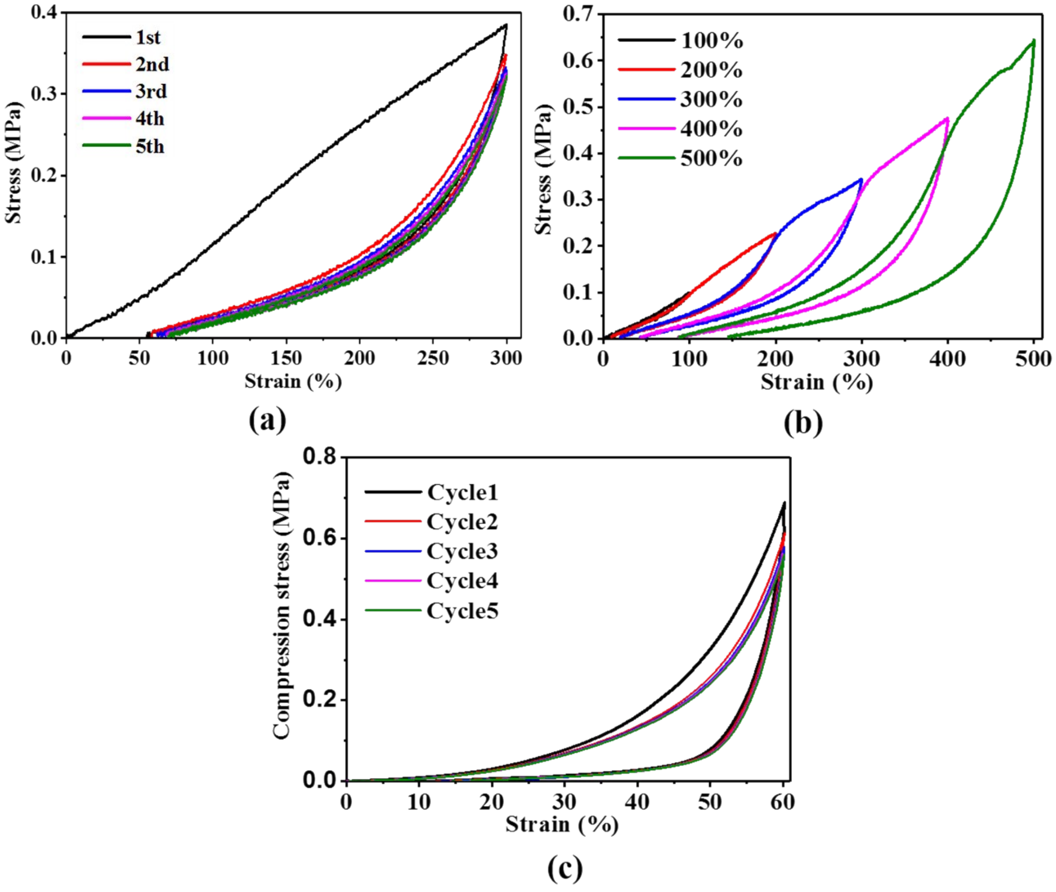

Figure S9 a) Successive cyclic tensile loading-unloading curves at 300% strain of pure PVA hydrogel for 5 cycles without resting time between each cycle; b) Cyclic compression loading-unloading curves of pure PVA hydrogel under different strains (100%, 200%, 300%, 400%, 500%); c) Typical continuous loading-unloading compression measurements of pure PVA hydrogel for 5 cycles at 60% strain without resting intervals.

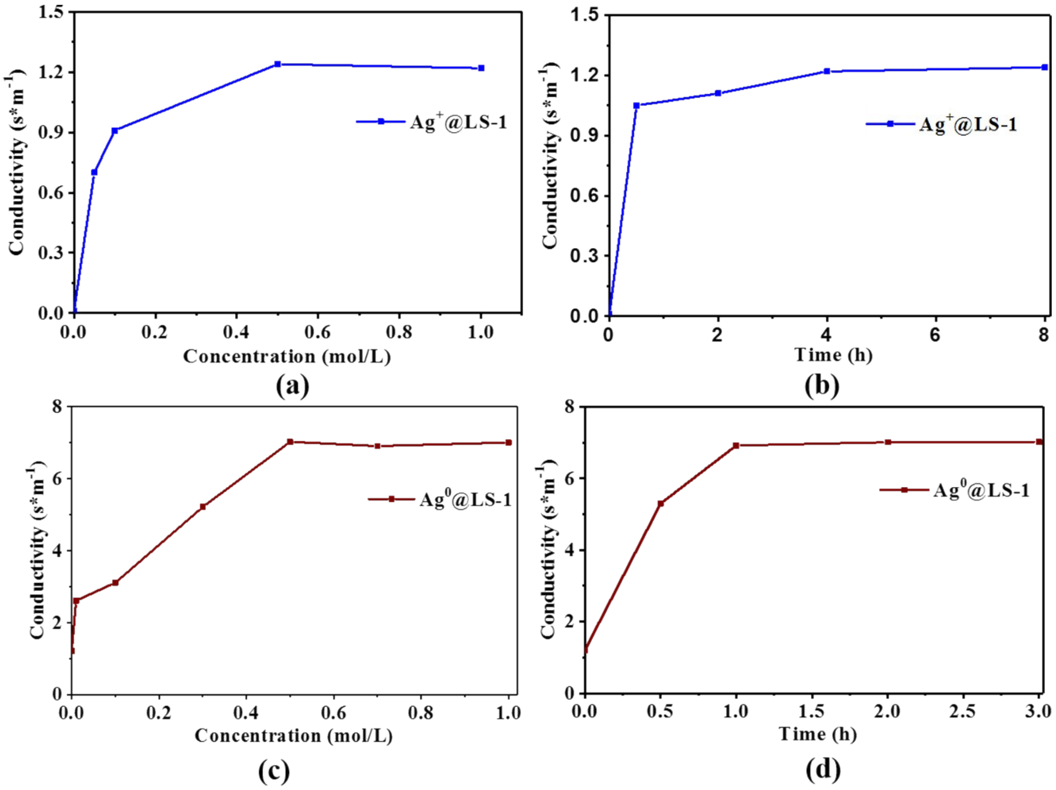

(a) (b) (c) (d)

Figure S10 a) Conductivity for Ag$^+$@LS-1 in different $AgNO_3$ concentrations with constant soaking time of 4 h; b) Conductivity for Ag$^+$@LS-1 at different soaking time in constant $AgNO_3$ concentration of 0.5 M; c) Conductivity for Ag^0@LS-1 in different $Na_3C_6H_5O_7$ concentrations with constant soaking time of 1 h; d) Conductivity for Ag^0@LS-1 at different soaking time in constant $Na_3C_6H_5O_7$ concentration of 1.0 M.

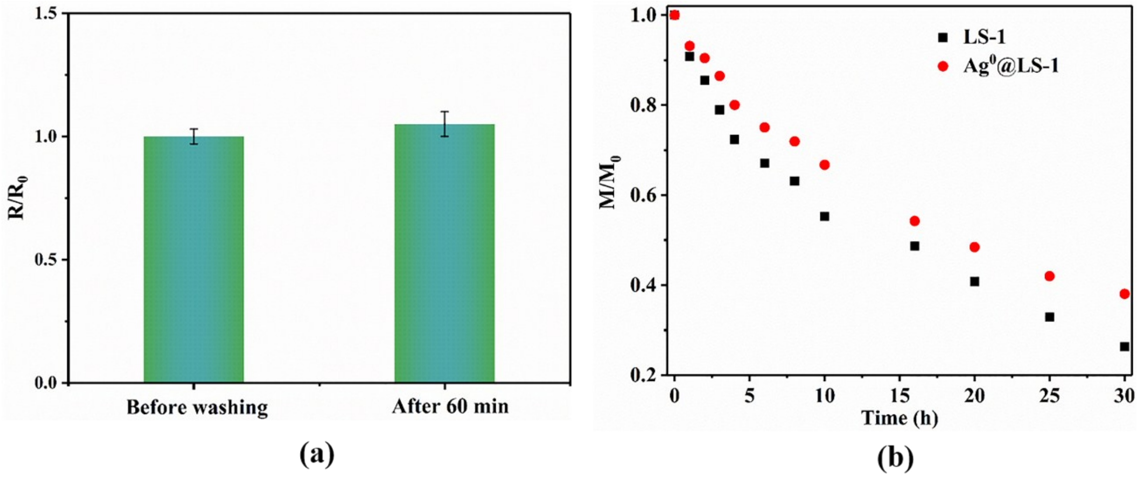

(a) (b)

Figure S11 a) Relative resistance change of Ag^0@LS-1 before and after washing with water; b) Comparison of weight loss for LS-1 and Ag^0@LS-1 in 55 °C air atmosphere.

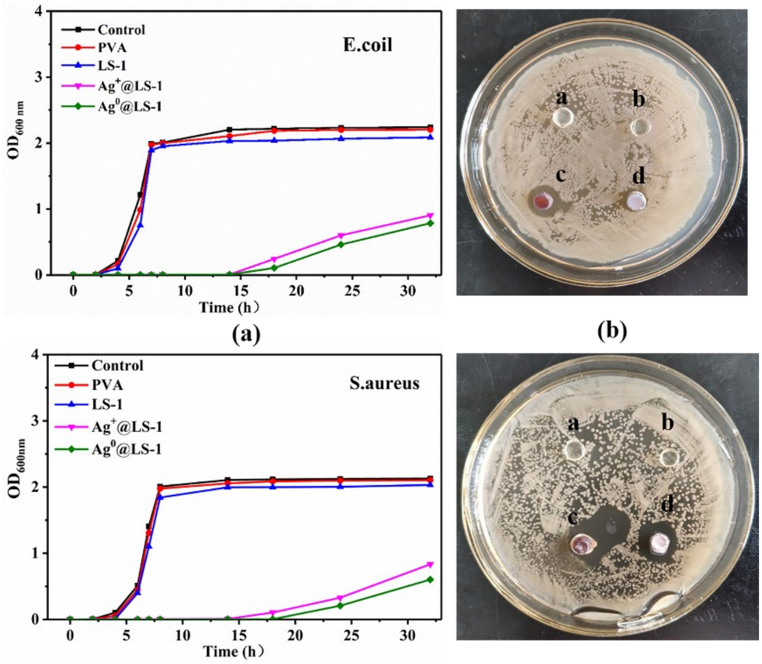

(a) (b)

(c) (d)

Figure S12 Growth curves of E. coli a) and S. aureus c) at different time intervals in the presence of different hydrogel samples; Bacteriostatic effect of composite hydrogels for (b) E.coil and (d) S. aureus after the hydrogels were washed for 30 min with water, (a. Pure PVA; b. LS-1; c. Ag^+@LS-1; d. Ag^0@LS-1).

The antibacterial activity of the hydrogel samples was evaluated against Gram-negative bacteria (E. coli) and Gram-negative bacteria (S. aureus). The microbial cells were treated by the hydrogel samples (10 mm in diameter and 3 mm in thickness), respectively. The cell growth curves were plotted against time according to the OD_{600nm} (Optical density at 600 nm recorded on a UV-visible spectrophotometer) after incubation. As shown in Figure S12, the composite hydrogels (Ag^+@LS-1 and Ag^0@LS-1) delayed the growth of E. coli and S. aureus obviously, and they could inhibit the growth of microbial cells for almost 15 h. In addition, Ag^+@LS-1 and Ag^0@LS-1 maintained excellent resistance stability and antibacterial property even after washing with water for 60 min (Figure S12b &d), suggesting that composite hydrogels (Ag^+@LS-1 and Ag^0@LS-1) exhibited good antibacterial durability. This was understandable as the Ag NPs in the composite hydrogel Ag^0@LS-1 were embedded in the tight hydrogel network, which were not that easy to leach rapidly.

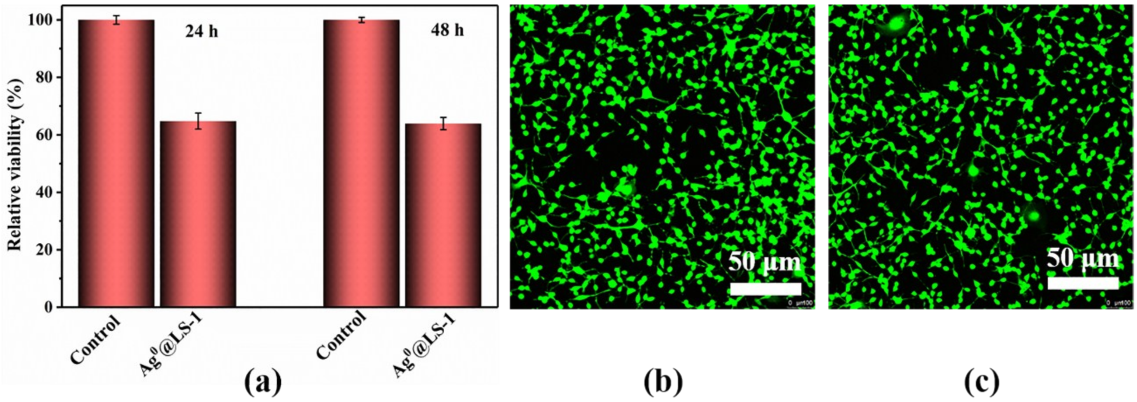

(a) (b) (c)

Figure S13 a) Relative viability of fibroblasts for the Ag^0@LS-1 hydrogel after 24 h and 48 h of culture (living cells without Ag^0@LS-1 was as control); b) Confocal laser scanning microscopy micrographs of fibroblasts adhered on Ag^0@LS-1 after 24 h and 48 h of culture (green fluorescence represented the Calcein-AM stained living cells).

Cytotoxicity of Ag^0@LS-1 were evaluated by MTT colorimetry methods and confocal laser scanning microscopy micrographs of fibroblasts.[3] Living cells without Ag^0@LS-1 was as control in the tests. As shown in Figure S13, relative viability of fibroblasts for the Ag^0@LS-1 hydrogel after 24 h and 48 h of culture was ~ 62%, suggesting the low toxicity of Ag^0@LS-1 towards fibroblasts. Confocal laser scanning microscopy micrographs of fibroblasts adhered on Ag^0@LS-1 presented the living fibroblasts cells after 24 h (Figure S13b) and 48 h (Figure S13c) culture.

Table S1. Mechanical properties of PVA and PVA composite hydrogels.

Sample	σ_t ^{a}	ε_t ^{a}	E_t ^{a}	τ_t ^{b}	σ_c ^{b}	τ_c ^{b}	*Conductiviy*

	[MPa]	[%]	[MPa]	[MJ/m^3]	[MPa]	[MJ/m^3]	(S/m)
PVA	0.62±0.05	461±13	0.06±0.01	1.12	6.39±0.06	0.75	0.009
LS-1	1.24±0.04	586±11	0.14±0.01	2.96	9.89±0.08	1.06	0.012
Ag$^+$@LS-1[c]	1.31±0.03	828±15	0.11±0.03	3.89	10.52±0.09	1.13	1.225
Ag^0@LS-1[d]	8.49±0.05	1285±8	1.80±0.02	50.71	18.61±0.05	1.50	7.124
Ag^0@LS-1[e]	5.87±0.02	875±13	0.42±0.01	20.92	14.51±0.03	1.32	5.164
Ag^0@PVA[f]	2.39±0.05	752±17	0.17±0.04	6.86	12.13±0.06	1.24	2.314

[a] Determined by tensile stress-strain curve, σ_t, ε_t, E_t, τ_t refer to the tensile stress, elongation at break, modulus and tensile toughness, respectively. [b] Determined by compression stress-strain curve, σ_c, and τ_c refer to the compression stress at 90% compression strain and compression toughness, respectively. [c] Ag$^+$@LS-1 was prepared by soaking LS-1 in 0.5 M $AgNO_3$ solution for 4 h. [d] Ag^0@LS-1was prepared by immersing Ag$^+$@LS-1 in 1.0 M $Na_3C_6H_5O_7$ solution for 1 h. [e] Ag^0@LS-1was prepared by immersing Ag$^+$@LS-1 in 1.0 M $Na_3C_6H_5O_7$ solution for 0.5 h. [f] Ag^0@PVA was prepared by soaking PVA hydrogel in 0.5 M $AgNO_3$ solution for 4 h and then in 1.0 M $Na_3C_6H_5O_7$ solution for 1 h.

REFERENCES

(1) X. Zhang, W. Liu, D. Yang, X.Qiu,. *Adv. Funct. Mater.* **2019**, *29*, 1806912.

(2) A. P. Richter, J. S. Brown, B. Bharti, A. Wang, S. Gangwal, K. Houck, E. A.Cohen Hubal, V. N. Paunov, S. D. Stoyanov, O. D. Velev, *Nat Nanotechnol*. **2015**, *10*, 817-823.

(3) D. Gan, T. Xu, W. Xing, X. Ge, L. Fang, K. Wang, F. Ren, X. Lu, *Adv. Funct. Mater.* **2019**, *29*, 1805964.